scientific reports

Check for updates

OPEN

Non-Markovian noise mitigation in quantum teleportation: enhancing fidelity and entanglement

Haiyang Zhang[1,2,3], Xiaoxiang Han[1,2,3], Guoqing Zhang[1,2,3], Lianbi Li[1,2,3], Lin Cheng[1,2,3], Jun Wang[1,2,3], Yunjie Zhang[1,2,3], Yanwen Xia[4] & Caijuan Xia[1,2,3]✉

Maintaining quantum coherence and entanglement in the presence of environmental noise, particularly within non-Markovian contexts, represents a significant challenge for the progression of quantum information science and technology. This study offers a substantial advancement by investigating the dynamics of a two-qubit system subjected to diverse noise conditions, encompassing relaxation, dephasing, and their cumulative effects. By employing quantum-state-diffusion equations specifically crafted for non-Markovian environments, we introduce an innovative strategy to counteract the detrimental influences of environmental noise on quantum teleportation fidelity and entanglement concurrence. Our results underscore the potential for external interventions to markedly improve the resilience of quantum information processing tasks over prolonged durations, especially in settings where dephasing noise prevails. A key revelation is the intricate relationship between dephasing noise and the initial state of entanglement, which profoundly impacts the occurrence of entanglement sudden death. This research not only deepens our comprehension of quantum system dynamics under noisy circumstances but also furnishes practical directives for engineering robust quantum systems, a necessity for the development of scalable quantum technologies.

Abbreviations

QSD	Quantum-state-diffusion
EPR	Einstein–Podolsky–Rosen
ESD	Entanglement sudden death
OU	Ornstein–Uhlenbeck

Quantum entanglement, a cornerstone of quantum mechanics, embodies the non-local correlations between quantum particles that challenge classical physics, famously critiqued by Einstein as "spooky action at a distance"[1–3]. This phenomenon is not merely a theoretical curiosity but serves as a fundamental resource in quantum information science, enabling revolutionary applications such as quantum teleportation, dense coding, cryptography, computing, and communications. However, the inherent openness of quantum systems to their environment exposes them to decoherence, a process that erodes entanglement and threatens the integrity of quantum information[4]. Decoherence is a critical challenge in quantum computing and quantum communication, as it can lead to the loss of quantum coherence and the degradation of quantum states.

Understanding the dynamics of quantum systems in the presence of environmental noise is crucial for the development of robust quantum technologies. In this context, it is important to distinguish between Markovian and non-Markovian processes. Markovian processes assume that the system's evolution is memoryless, i.e., independent of its past, whereas non-Markovian processes account for memory effects, with the system's evolution depending on its history. In environments with pronounced memory effects, such as structured environments where the correlation time of the environment is comparable to the system's time scale, non-Markovian approximations are more suitable for describing the decoherence process[5–9]. The Markovian approximation, while useful in many scenarios, fails to accurately capture the dynamics in such environments, necessitating the use of non-Markovian models to describe the system's evolution. Even in relatively isolated systems, entanglement loss remains a persistent challenge due to unavoidable interactions with auxiliary systems or interfaces that are essential for the storage, evolution, reading, and coherent manipulation of quantum states.

[1]School of Science, Xi'an Polytechnic University, No. 19 Jinhua South Road, Xi'an 710048, Shaanxi, China. [2]Engineering Research Center of Flexible Radiation Protection Technology, Universities of Shaanxi Province, Xi'an Polytechnic University, Xi'an 710048, Shaanxi, China. [3]Xi'an Key Laboratory of Nuclear Protection Textile Equipment Technology, Xi'an Polytechnic University, Xi'an 710048, Shaanxi, China. [4]4Research Center of Laser Fusion, Chinese Academy of Engineering Physics (CAEP), Mianyang 621900, China. ✉email: cjuanxia@163.com

These interactions, albeit necessary, introduce noise that can corrupt quantum information, making it imperative to operate under conditions that minimize external noise interference[10,11]. The challenge lies in maintaining the delicate balance between the necessity of these interactions and the detrimental effects of environmental noise.

To counteract the adverse effects of environmental noise, several strategies have been developed, including quantum error correction, decoherence-free subspaces, and dynamical decoupling[12–20]. Quantum error correction employs redundant encoding to detect and correct errors, while decoherence-free subspaces leverage symmetries in the system-environment interaction to protect quantum states. Dynamical decoupling, conversely, uses fast, periodic control pulses to suppress the interaction between the quantum system and its environment, effectively "decoupling" the system from the noise. In this landscape, quantum teleportation emerges as a groundbreaking process that enables the transfer of quantum states between distant parties without the physical transmission of particles. This phenomenon relies on quantum entanglement and classical communication[21]. In this process, two parties, typically referred to as Alice and Bob, share a pair of entangled particles. When Alice wishes to teleport a quantum state, she performs a joint measurement on her particle and the state to be teleported, collapsing the system into one of several possible outcomes. This measurement generates classical information, which Alice sends to Bob. Upon receiving this information, Bob applies a corresponding unitary operation to his entangled particle, effectively reconstructing the original quantum state. However, the implementation of quantum teleportation is enhanced by addressing the challenges posed by non-Markovian noise, which can degrade the fidelity and entanglement of the teleported state. Non-Markovian noise refers to memory effects in the environment that influence the dynamics of quantum systems over time, leading to complex interactions inadequately described by Markovian models[22,23]. The proposed mitigation strategies include advanced error correction techniques and adaptive protocols that dynamically respond to the noise characteristics during the teleportation process. By incorporating these strategies, the model aims to improve the robustness of quantum teleportation against environmental disturbances, thereby enhancing the overall fidelity of the teleported states and preserving the entanglement between the particles[24,25]. This advancement is crucial for developing reliable quantum communication networks and quantum computing systems, where maintaining high fidelity and entanglement is essential for practical applications.

In complex systems where multiple noise sources coexist, the interplay between these noises can either enhance or suppress coherence, internal correlations, and entanglement. This paper introduces an innovative approach to controlling non-Markovian relaxation processes through a Markovian dephasing process[26–30]. By harnessing this phenomenon, it becomes feasible to manipulate the impact of noise on the system via controlled noise sources[31–37]. This control strategy is akin to sculpting the noise landscape to favor the preservation of quantum information, guiding a quantum system through a noisy environment while maintaining its quantum coherence and entanglement. A significant body of research has been dedicated to understanding the dynamics of entanglement in quantum systems, often quantified by Wootters' concurrence[38–41]. Most studies have focused on two-qubit atomic systems under the Markovian approximation. However, our investigation delves into the optimization of quantum teleportation and the evolution of entanglement dynamics by blending noises from two distinct environments for two-qubit atomic systems under the non-Markovian approximation. We employ the quantum-state-diffusion approach to solve the master equations for non-Markovian processes, elucidating how different noise mixtures influence quantum teleportation and entanglement dynamics. This approach allows us to visualize the intricate interplay between noise and quantum information, revealing strategies to enhance the robustness of quantum systems against environmental decoherence. By understanding how to blend and control noise sources, we can potentially improve the fidelity of quantum operations and the stability of quantum states.

The paper is structured as follows. The physical model section outlines the mathematical model for our system and details the non-Markovian quantum-state-diffusion method. Results section presents the numerical results of fidelity for a range of noise strengths and memory capacities, as well as an analysis of entanglement dynamics for varying noise parameters. Finally, conclusions section summarizes our findings, highlighting the implications for the control and preservation of quantum information in noisy environments.

The physical model

Two-qubit model

In the ensuing work, we delve into a two-qubit system wherein each qubit autonomously interacts with its respective local environment, as visualized in Fig. 1.

The two atoms, positioned within their individual local environments, are sufficiently distant to prevent any direct interaction, with the exception of the initial quantum entanglement that connects them. Within this system, we employ the non-Markovian quantum-state-diffusion (QSD) methodology to obtain the exact solution of the model, accounting for both relaxation and dephasing noise phenomena[8,42,43]. The Hamiltonian can be expressed as follows ($\hbar = 1$)

$$\mathscr{H}_{tot} = \mathscr{H}_{sys} + \mathscr{H}_{env} + \mathscr{H}_{int}, \tag{1}$$

where

$$\mathscr{H}_{sys} = \frac{1}{2}\left(\omega_A \sigma_z^A + \omega_B \sigma_z^B\right), \tag{2}$$

$$\mathscr{H}_{env} = \sum_k \left(\omega_{Ak} b_k^{A\dagger} b_k^A + \omega_{Bk} b_k^{B\dagger} b_k^B\right) \tag{3}$$

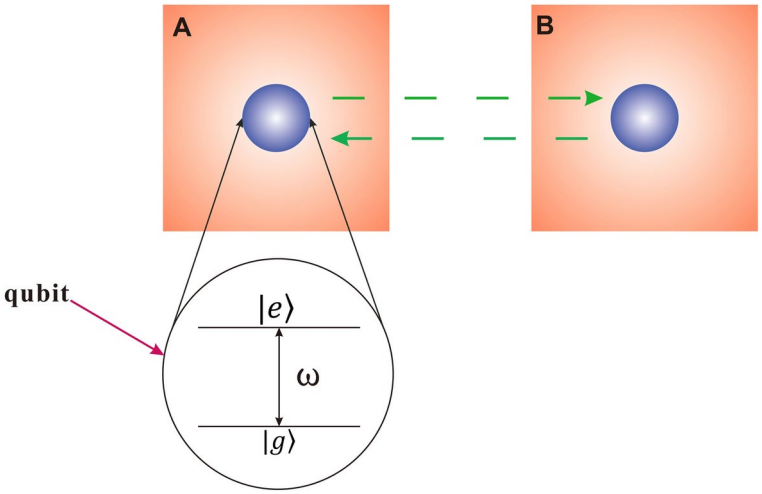

Fig. 1. The entangled state of two separate 2-level atoms is illustrated in the schematic diagram. Initially, qubits A and B each independently interact with their respective local environments, maintaining their quantum coherence without direct coupling.

$$\mathscr{H}_{int} = \frac{1}{2}\left[\xi(t)\sigma_z^A + \xi(t)\sigma_z^B\right] + \left(\sigma_-^A B_A^\dagger + h.c.\right) + \left(\sigma_-^B B_B^\dagger + h.c.\right). \tag{4}$$

In the heart of the model lie the isolated system's Hamiltonian, $\mathscr{H}_{sys}$, and the environment's Hamiltonian, $\mathscr{H}_{env}$. Their interaction is encapsulated within $\mathscr{H}_{int}$. Notable quantities include the qubit frequencies ω_A and ω_B associated with qubits A and B, respectively, alongside the Pauli matrices σ_z and the raising operator $\sigma_- = (\sigma_x - i\sigma_y)/2$. Dephasing noise, characterized by $\xi(t)$, contributes to the dynamics. Environmental modes are represented by annihilation operators b_k and eigenfrequencies ω_k. The relaxation channels for each qubit are defined by collective operators: $B_A = \sum_k g_{Ak} b_k^A$ for qubit A and $B_B = \sum_k g_{Bk} b_k^B$ for qubit B, with g_{Ak} and g_{Bk} representing coupling strengths to respective modes.

Utilizing a time-varying unitary transformation $U = \exp\left[-i\left(\mathscr{H}_{env}t + \frac{1}{2}\left[\Xi(t)\sigma_z^A + \Xi(t)\sigma_z^B\right]\right)\right]$ and the integral $\Xi(t) = \int_0^t ds\xi(s)$, which captures the cumulative effect of environmental noise over time, the total Hamiltonian in the rotating frame can be reformulated accordingly as

$$\begin{aligned}\mathscr{H}_{rot} &= U^+\mathscr{H}_{tot}U - iU^+\frac{dU}{dt} \\ &= \mathscr{H}_{sys} + \sigma_-^A B_A^\dagger(t)e^{-i\Xi(t)} + \sigma_+^A B_A(t)e^{i\Xi(t)} + \sigma_-^B B_B^\dagger(t)e^{-i\Xi(t)} + \sigma_+^B B_B(t)e^{i\Xi(t)}.\end{aligned} \tag{5}$$

The time-domain representations of the collective operators A and B can be expressed as follows:

$$\begin{aligned}B_A(t) &= \sum_k g_{Ak} b_k^A e^{-i\omega_{Ak}t} \\ B_B(t) &= \sum_k g_{Bk} b_k^B e^{-i\omega_{Bk}t}.\end{aligned} \tag{6}$$

Both equations describe the complex sinusoidal components (denoted by b_k^A and b_k^B, each weighted by their respective coefficients g_{Ak} and g_{Bk}, and oscillating at angular frequencies ω_{Ak} and ω_{Bk}) that make up the overall operators B_A and B_B as functions of time t.

Non-Markovian QSD method

In the framework of the QSD approach, one can project all of the environment modes onto the Bargmann coherent states $||z\rangle = \sum_{n=0}^{\infty} \frac{z^n}{\sqrt{n!}}|n\rangle$. As we know, the full state wave function of the system and the environment $|\psi_{tot}(t)\rangle$ should satisfy the Schrödinger equation

$$\partial_t|\psi_{tot}(t)\rangle = -i\mathscr{H}_{rot}|\psi_{tot}(t)\rangle. \tag{7}$$

It is difficult to solve for the wave function directly due to the presence of environmental degrees of freedom. Therefore, the completeness of coherent states needs to be utilized to reduce the environmental degrees of freedom as

$$|\psi_{tot}(t)\rangle = \int \frac{d^2z}{\pi}e^{-|z|^2}||z\rangle\langle z||\cdot|\psi_{tot}(t)\rangle, \tag{8}$$

where the Bargmann coherent states $||z\rangle = ||z_1\rangle \otimes ||z_2\rangle \otimes ||z_3\rangle \otimes \cdots ||z_k\rangle \otimes \cdots$ and $||z_k\rangle$ represents the stochastic variable of fluctuation of the kth mode of the environment. Since the Bargmann coherent state is complete, this set of stochastic variables is consistent with a Gaussian distribution. We can represent the complex effects of the environment through Gaussian noise. Therefore, the state vector of the two-qubit system can be projected onto the Bargmann coherent states as follows:

$$|\psi_t(z^*)\rangle = \langle z|| \cdot ||\psi_{tot}(t)\rangle . \tag{9}$$

By a straightforward derivation, projecting Schrödinger's equation to the stochastic state $||z\rangle$, we can obtain a formal QSD equation

$$\frac{\partial}{\partial t}\psi_t(z^*) = \left[-i\mathscr{H}_{sys} + L_A z_{At}^* + L_B z_{Bt}^* - L_A^\dagger \bar{O}_A(t, z^*) - L_B^\dagger \bar{O}_B(t, z^*)\right]\psi_t(z^*), \tag{10}$$

where $\bar{O}_i(t, z^*) \equiv \int_0^t ds G_i(t-s) O_i(t, s, z^*)$ (where $i = A, B$) are defined as system operators that incorporate time integration. This indicates that the system's evolution is influenced by both the current and historical states of the environment, a characteristic of non-Markovian processes, in contrast to Markovian processes, which depend solely on the present state. These operators are intrinsically linked to the coupling between the system and the environment through the system operators $O_i(t, z^*)$ and coupling operators L_i (e.g., σ_-^A and σ_-^B). This relationship emphasizes that the system's dynamics are governed not only by its Hamiltonian $\mathscr{H}_{\text{sys}}$ but also by its interactions with the environment. In quantum teleportation and other quantum information tasks, these operators are crucial for quantifying the impact of environmental noise on system performance. By analyzing and controlling these terms, strategies can be developed to mitigate noise effects, thereby enhancing fidelity and entanglement in quantum communication and computation. The operator $O_i(t, s, z^*)$ is derived from the equation

$$\frac{\delta\psi_t(z^*)}{\delta z_{it}^*} = O_i(t, s, z^*)\psi_t(z^*). \tag{11}$$

Since these two qubits are in the equivalent environment, they exhibit the same form of combined correlation function. For environmental noise $z_{it}^* = -i\sum_k g_{ik}^* z_k^* e^{i\omega_{ik}t - i\Xi_i(t)}$, the correlation function $G_i(t-s)$ can be written as

$$\begin{aligned} G_i(t-s) &= \mathscr{M}[z_{it}^* z_{is}^*] \\ &= \sum |g_k^2| e^{i[\Xi(t)-\Xi(s)]-i\omega_k(t-s)} \\ &= \beta(t-s)\left[-\int_0^t dt_1 \int_0^t dt_2 \alpha(t_1 - t_2)\right], \end{aligned} \tag{12}$$

where $\omega_k = \omega_{Ak} = \omega_{Bk}$, $g_k = g_{Ak} = g_{Bk}$, $\Xi = \Xi_A = \Xi_B$ and $\mathscr{M}[\cdot] = \int \frac{d^2z}{\pi} e^{-|z|^2}$ means an ensemble average. For both two qubits, $\alpha(t-s) = \frac{\Gamma_\alpha \gamma_\alpha}{2} e^{-\gamma_\alpha |t-s|}$ and $\beta(t-s) = \frac{\Gamma_\beta \gamma_\beta}{2} e^{-\gamma_\beta |t-s|}$ represent Ornstein–Uhlenbeck (OU) noise correlation functions of dephasing and relaxation noise, respectively. γ_α and γ_β are inverse memory capacities of the relevant noise. For a long system-environment memory, the backflow of information into the quantum systems delays the decoherence between the qubits. Γ_α and Γ_β are the coupling strengths between the qubits and their environments, respectively. Therefore, the combined noise correlation function can be expressed as

$$G_i(t-s) = \frac{\Gamma_\beta \gamma_\beta}{2} e^{-\gamma_\beta |t-s|} \exp\left\{-\frac{\Gamma_\alpha}{2}\left[(t-s) + \frac{e^{-\gamma_\alpha(t-s)} - 1}{\gamma_\alpha}\right]\right\}. \tag{13}$$

Obviously, the combined correlation function $G_i(t-s)$ no longer maintains the form of linear exponential decay and the combination of two OU noise sources will not yield another OU noise. However, if one of them is under Markovian approximation, e.g., when $\gamma_\alpha \to \infty$ the correlation function of the dephasing noise becomes $\alpha(t-s) = \Gamma_\alpha \delta(t-s)$. By using the above conditions, the combined correlation function $G_i(t-s)$ reduces to

$$G_i(t-s) = \frac{\widetilde{\Gamma}_\beta \widetilde{\gamma}_\beta}{2} \exp\left[-\widetilde{\gamma}_\beta |t-s|\right], \tag{14}$$

where, $\widetilde{\Gamma}_\beta = r\Gamma_\beta$, $r = \gamma_\beta/\widetilde{\gamma}_\beta$ and $\widetilde{\gamma}_\beta = \gamma_\beta + \Gamma_\alpha/2$. Since the fact that the coupling strength of noise $\widetilde{\Gamma}_\beta < \Gamma_\beta$ and $\widetilde{\gamma}_\beta > \gamma_\beta$, it is not difficult to observe the important difference between the combined noise correlation function and the pure non-Markovian relaxation noise correlation function. Due to the fact that the non-Markovian memory capacities γ_α and γ_β for relaxation and dephasing noises are from separable distinct sources, the competition between these two sources produces interesting behaviors in the control dynamics. Then, we bring Eq. (11) into the "consistency condition" $\frac{\delta}{\delta z_{it}^*}\frac{\partial \psi_t(z^*)}{\partial t} = \frac{\partial}{\partial t}\frac{\delta \psi_t(z^*)}{\delta z_{it}^*}$ to obtain the time evolution equation of the operator $O_i(t, s, z^*)$ shown as

$$\frac{\partial}{\partial t}O_i\left(t,s,z^*\right)=\left[-\frac{i}{2}\omega\sigma_z^i+L_iz_{it}^*-L_i^\dagger\bar{O}_i\left(t,z^*\right)O_i\left(t,s,z^*\right)\right]-L_i^\dagger\frac{\delta}{\delta z_{it}^*}\bar{O}_i\left(t,z^*\right). \tag{15}$$

As a result, by tackling the given equation, we obtain the proper expression for the operator $O_i\left(t,s,z^*\right)$. When dealing with two-qubit systems in dissipative scenarios, both $O_i\left(t,s,z^*\right)$ and its counterpart $\bar{O}_i\left(t,z^*\right)$ can be retained in their respective straightforward forms

$$\begin{aligned}O_i\left(t,s,z^*\right)&=f_i\left(t,s\right)\sigma_-^i,\\ \bar{O}_i\left(t,z^*\right)&=F_i\left(t\right)\sigma_-^i.\end{aligned} \tag{16}$$

The integral form of the equation for $F_i(t)$ is given by:

$$F_i(t)=\int_0^t G_i(t-s)f_i(t,s)\,ds. \tag{17}$$

Here, the coefficient function $f_i(t,s)$ must satisfy certain conditions or properties, which are not specified in this excerpt. To provide a complete statement, it may be necessary to include information about those constraints or the relationship it bears with $G_i(t)$ and $F_i(t)$. For example: $f_i(t,s)$ must adhere to specific mathematical rules, such as being continuous or differentiable, to ensure the solvability of the integral and the well-definedness of the function $F_i(t)$,

$$\partial_t f_i\left(t,s\right)=\left(i\omega+F_i\left(t\right)\right)f_i\left(t,s\right). \tag{18}$$

To calculate $F_i(t)$ efficiently, we typically work with the master equation derived from the QSD Eq. (10). Starting with the density matrix $\rho(t,z^*)=|\psi_t(z^*)\rangle\langle\psi_t(z^*)|$ including noise, the system's final density matrix $\rho_s(t)=\mathscr{M}\left[\rho(t,z^*)\right]$ is obtained by averaging over all noise realizations. By applying Novikov's theorem[42,44,45] in conjunction with the QSD equation, the master equation is then derived

$$\begin{aligned}\dot{\rho}_s\left(t\right)=&-i\left[\frac{\omega}{2}\left(\sigma_z^A+\sigma_z^B\right),\rho_s\right]\\&+F_{AR}(t)\left(2\sigma_-^A\rho_s\sigma_+^A-\sigma_+^A\sigma_-^A\rho_s-\rho_s\sigma_+^A\sigma_-^A\right)\\&+F_{BR}(t)\left(2\sigma_-^B\rho_s\sigma_+^B-\sigma_+^B\sigma_-^B\rho_s-\rho_s\sigma_+^B\sigma_-^B\right).\end{aligned} \tag{19}$$

In the equation, $F_{AR}(t)$ represents the real part of $F_A(t)$, while $F_{BR}(t)$ corresponds to the real part of $F_B(t)$. The system's initial state is considered a pure state expressed as:

$$|\Psi_0\rangle=\alpha_1|1\rangle+\alpha_2|2\rangle+\alpha_3|3\rangle+\alpha_4|4\rangle.$$

Here, the basis kets correspond to: $|1\rangle=|e_Ae_B\rangle$, $|2\rangle=|e_Ag_B\rangle$, $|3\rangle=|g_Ae_B\rangle$, and $|4\rangle=|g_Ag_B\rangle$. Each amplitude α_i, where i ranges from 1 to 4, denotes the probability amplitude of the state $|i\rangle$, satisfying the normalization condition $\sum_{i=1}^4|\alpha_i|^2=1$.

Results

Fidelity control

In the endeavor to perfect quantum teleportation, it is imperative to evaluate the discrepancy between the actual and ideal quantum information transmission. To this end, we introduce a distance metric $\mathscr{F}\equiv\left|\langle\Psi_2|\,\Psi_1\rangle\right|^2$, which quantifies the degree of overlap between a state $|\Psi_1\rangle$ and a reference state $|\Psi_2\rangle$. This metric serves as a measure of the quantum coherence and fidelity between the two states. By employing the exact equation of motion (Eq. 19) and the initial state $|\Psi_0\rangle$, the fidelity can be mathematically formulated as $\mathscr{F}\left(t\right)\equiv\langle\Psi_0|\,\rho_s\left(t\right)|\Psi_0\rangle$. In quantum information theory, fidelity is not merely a measure of similarity between quantum states but also a critical indicator of the quality of information transmission in quantum communication. Specifically, the fidelity directly reflects the extent of noise affecting the quantum state during transmission; a fidelity of 1 indicates perfect transmission, while a fidelity close to 0 signifies nearly complete information loss. Therefore, analyzing fidelity allows us to gain deeper insights into the impact of environmental noise on quantum states and provides a theoretical basis for optimizing quantum transmission processes. Moreover, variations in fidelity can reveal the dynamic behavior of the system across different time scales, helping us identify effective strategies to enhance the stability and transmissibility of quantum states in non-Markovian noise environments. EPR systems, named after the influential paper by Einstein, Podolsky, and Rosen, are fundamental to quantum communication, utilizing quantum entanglement to create correlated particle pairs. This property allows the state of one particle to instantaneously influence the state of another, regardless of distance, which is crucial for secure quantum communication protocols like quantum key distribution. However, EPR systems face challenges from environmental interactions that can lead to decoherence, degrading entangled states. To investigate this, the analysis begins with a Bell state as the initial state of the system, represented as: $|\Psi_0\rangle=\frac{1}{\sqrt{2}}\left(|2\rangle+|3\rangle\right)$. This Bell state is one of four maximally entangled states, characterized by symmetry and equal probability of measuring either qubit in the states $|2\rangle$ and $|3\rangle$. By studying the effects of environmental interactions on this state, insights into the resilience of quantum communication systems against decoherence can be gained, which is essential for enhancing their reliability and security.

To explore the impact of inversion memory capacity γ_β (spanning from 0.1 to 2) on the dynamics of entanglement during quantum teleportation, we performed a numerical evaluation of the fidelity, as illustrated in Fig. 2. Each graph maintains a constant noise intensity for the relaxation process, while dephasing noise of varying intensities is applied to the respective environments. The black solid line, labeled R, signifies the fidelity of the qubit system under pure relaxation noise, while the blue lines, labeled C, represent the fidelity in the presence of both relaxation and dephasing noise. Distinct line styles on the blue curves denote different strengths (decoherence rates) of the dephasing noise. The inset in each panel of Fig. 2 depicts the evolution of the probability amplitudes of the ground state $|4\rangle = |g_A g_B\rangle$. The three graphs in Fig. 2 are arranged in ascending order of γ_β, corresponding to a decreasing memory capacity for relaxation noise. For a long system-environment memory time ($\gamma_\beta/\omega = 0.1$), Fig. 2a clearly demarcates two regions: one dominated by pure relaxation noise (black curve) and the other by mixed noises with varying dephasing rates Γ_α. In the moderate-time scale ($0 < \omega t < \tau$, where τ is the critical time marking the intersections of the black curve and the blue curves), the fidelity under mixed noises is observed to surpass that under pure relaxation noise. Importantly, a higher dephasing strength Γ_α results in a longer critical time and higher fidelity, indicating that our noise control strategy can enhance fidelity under short-time constraints.

In Fig. 2b, for a moderate system-environment memory time ($\gamma_\beta/\omega = 0.5$), the black curve exhibits a more rapid decline compared to the previous scenario. Notably, for a significant dephasing strength ($\Gamma_\alpha/\omega = 4$), the critical time experiences a substantial increase. Figure 2c demonstrates the scenario involving relaxation noise with a short system-environment memory ($\gamma_\beta/\omega = 2$) and dephasing noise. It is evident that the effective decay rate based on relaxation noise can be consistently mitigated by the addition of dephasing noise. The inset in Fig. 2 reveals the evolution of the probability amplitude P_{gg} of the state $|4\rangle$. A clear correlation between the fidelity and P_{gg} is observed, suggesting that the loss of fidelity is directly associated with the decay of the two qubits from a Bell state $|\Psi_0\rangle$ to a ground state $|g_A g_B\rangle$. This observation underscores the significance of managing environmental interactions to preserve quantum information during teleportation processes, highlighting the potential benefits of strategic noise control in enhancing the fidelity of quantum state transfer. This insight not only emphasizes the need for precise environmental control but also opens avenues for developing more robust quantum communication protocols, which could potentially lead to advancements in quantum computing and cryptography, thereby contributing to the broader field of quantum information science. Given that the two qubits are situated in distinct environments (A) and (B), we investigated a scenario where dephasing noise is localized to only one environment (specifically, ($\Gamma_{B\alpha}/\omega = 0$)). The fidelities for these distinct noise scenarios, under four varying dephasing strengths ($\Gamma_{A\alpha}$) in environment (A), are analyzed numerically and visualized in Fig. 3. The black solid curve, marked with R, delineates the fidelity of the qubit system under the influence of pure relaxation noise alone. In contrast, the four curves labeled C represent the composite noise processes, which include both relaxation and dephasing effects.

In a moderate-time scale ($0 < \omega t < \tau$), where ($3.2 < \tau < 4.5$) as depicted in Fig. 3, the fidelity under mixed noises in environment (A) is observed to be superior to that under only purely relaxation noise in both environments (A) and (B). This can be attributed to the reduced complexity of noise interactions in a single environment, which effectively shields the qubit system from the more severe degradation of coherence that would otherwise occur under dual environmental noise. The single-noise environment scenario allows for a more controlled interaction between the qubit and its environment, leading to a slower decay of coherence. A comparison between Figs. 2a and 3 reveals that the critical time (τ)-the pivotal moment at which the fidelity starts to markedly deteriorate-when dephasing noise is present in both environments is extended compared to when it is confined to a single environment. This extension of the critical time can be further understood through the lens of non-Markovian effects, which become particularly pronounced in the presence of memory-intensive noise processes. Non-Markovianity implies that the system's evolution is not only dependent on its current state but also on its history of interactions with the environment. In our case, the system's exposure

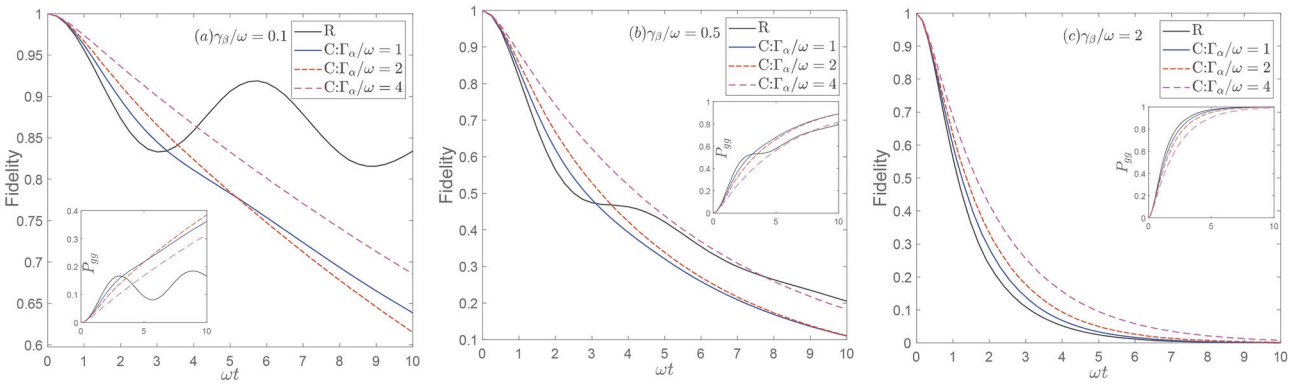

Fig. 2. The fidelity of the teleportation of two 2-level atoms system, where the relaxation noise and the dephasing noise are both present in their respective environments. Here R and C represent the dynamics under pure relaxation noise and a mixture of noises. The inset figure indicates the evolution of probability amplitudes P_{gg} of the state $|4\rangle$. We choose other parameters as $\Gamma_\alpha/\omega = \Gamma_{A\alpha}/\omega = \Gamma_{B\alpha}/\omega$, $\Gamma_\beta/\omega = \Gamma_{A\beta}/\omega = \Gamma_{B\beta}/\omega = 1$, $\gamma_\beta/\omega = \gamma_{A\beta}/\omega = \gamma_{B\beta}/\omega = (a)0.1, (b)0.5$ and $(c)2$.

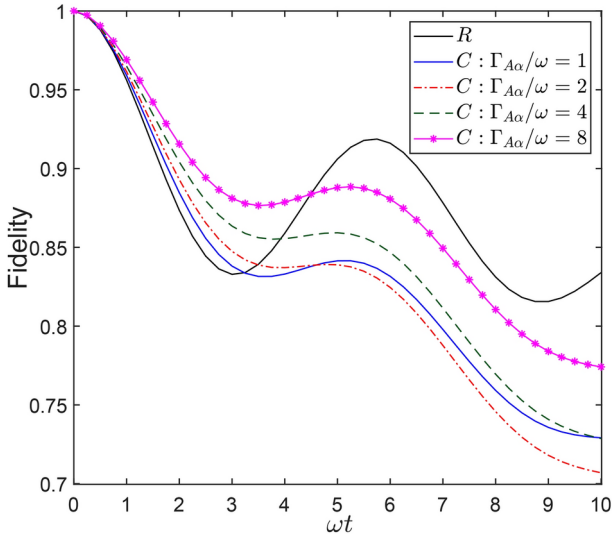

Fig. 3. The fidelity of the teleportation of two 2-level atoms system, where the relaxation noise and the dephasing noise are both present in their respective environments. Here R and C represent the dynamics under pure relaxation noise and the mixture of noises, respectively. We choose $\Gamma_\beta/\omega = \Gamma_{A\beta}/\omega = \Gamma_{B\beta}/\omega = 1$, $\gamma_\beta/\omega = \gamma_{A\beta}/\omega = \gamma_{B\beta}/\omega = 0.1$ and $\Gamma_{B\alpha}/\omega = 0$.

to noise in both environments leads to a more gradual loss of fidelity initially, as the noise correlations exhibit memory, causing temporary coherence revivals. These revivals are indicative of the system's ability to 'remember' and potentially reverse some of the noise-induced degradation, a characteristic signature of non-Markovian dynamics. However, in the region where ($\omega t > \tau$), the fidelity decays at a slower pace when dephasing noises are restricted to a single environment, suggesting that the system has adapted to the noise, leading to a stabilization of the fidelity decay rate. In contrast, the system subjected to noise in both environments continues to experience a more pronounced decay due to the cumulative effect of noise from both sides. The non-Markovian nature of the noise in this scenario implies that the system's coherence is not only affected by the immediate noise but also by the historical influence of the noise, which can lead to a more complex interplay between the system and its environment. These underscore the critical role of understanding the distribution and nature of environmental noise sources in preserving the coherence and fidelity of quantum systems. This is particularly crucial in the context of quantum computing and information processing, where maintaining qubit coherence is essential for reliable quantum operations. Understanding and controlling environmental noise, especially non-Markovian noise, is a key challenge in advancing quantum technologies. Strategic manipulation of the noise environment could potentially enhance qubit performance by exploiting memory effects to prolong coherence times, thereby advancing the field of quantum computing.

Entanglement dynamics

To further illuminate the temporal evolution of entanglement within our quantum system, we leverage Wootters' concurrence as a pivotal metric. This measure, specifically designed for a two-qubit system, is mathematically defined as:

$$C = \mathrm{Max}\left\{0, \sqrt{\lambda_1} - \sqrt{\lambda_2} - \sqrt{\lambda_3} - \sqrt{\lambda_4}\right\}, \tag{20}$$

where $\lambda_i (i = 1, 2, 3, 4)$ are the eigenvalues, arranged in descending order, of the matrix

$$M = \rho_s(t)\left(\sigma_y \otimes \sigma_y\right)\rho_s^*(t)\left(\sigma_y \otimes \sigma_y\right), \tag{21}$$

with $\rho_s^*(t)$ denoting the complex conjugate of $\rho_s(t)$ and σ_y being one of the Pauli matrices. The concurrence ranges from $C = 0$, indicating a separable state, to $C = 1$, representing a maximally entangled state.

A deeper examination of the matrix M and its eigenvalues λ_i reveals that these eigenvalues are derived by applying the operation $(\sigma_y \otimes \sigma_y)$ to the density matrix $\rho_s(t)$ and its complex conjugate. This operation flips the sign of the off-diagonal elements, which is crucial for coherence terms. The eigenvalues λ_i are the roots of a quartic polynomial, real, non-negative, and ordered in descending order. Their physical significance lies in their relation to the purity of the quantum state: the sum of the eigenvalues equals the trace of M, which also equals the trace of $\rho_s(t)$. Given that the trace of a density matrix is always 1, the sum of the eigenvalues of M is also 1, implying they can be interpreted as probabilities of measuring specific states.

Entanglement is directly linked to these eigenvalues. The concurrence C quantifies the degree of correlation between the two qubits. A separable state, characterized by $C = 0$, occurs when the eigenvalues of M are all equal, suggesting the state can be described as a product of two individual qubit states. Conversely, a maximally entangled

state, with $C = 1$, occurs when one eigenvalue of M is 1 and the others are 0, indicating a superposition of two orthogonal qubit states with equal probability amplitudes. The eigenvalues of the matrix M and the concurrence C provide a robust framework for understanding the entanglement of quantum states. The concurrence C offers a quantitative measure of entanglement, enabling comparisons between different quantum states and tracking the evolution of entanglement over time. This is crucial for enhancing the fidelity and entanglement in quantum teleportation protocols, particularly in the context of non-Markovian noise mitigation strategies.

In our subsequent analysis, we concentrate on the temporal dynamics of entanglement under various initial conditions, focusing on the Bell states

$$|\Psi_0\rangle = \cos(\theta/2)\,|2\rangle + \sin(\theta/2)e^{i\phi}\,|3\rangle$$

and

$$|\Phi_0\rangle = \cos(\theta/2)\,|1\rangle + \sin(\theta/2)e^{i\phi}\,|4\rangle\,.$$

By calculating the density matrix $\rho_s(t)$ and substituting it into Eq. 21, we can track the evolution of the concurrence over time. It is imperative to note that the initial states are characterized by the parameters θ and ϕ. A critical aspect of our investigation is the influence of different initial states and dephasing rates Γ_α on the entanglement dynamics of the atomic system.

In Fig. 4, we depict the time evolution of the concurrence as a function of ωt and θ for the initial states $|\Psi_0\rangle$ and $|\Phi_0\rangle$. Our observations reveal that entanglement sudden death (ESD), a phenomenon where entanglement abruptly ceases to exist, is a characteristic feature for the initial state $|\Phi_0\rangle$, with the ESD time being dependent on

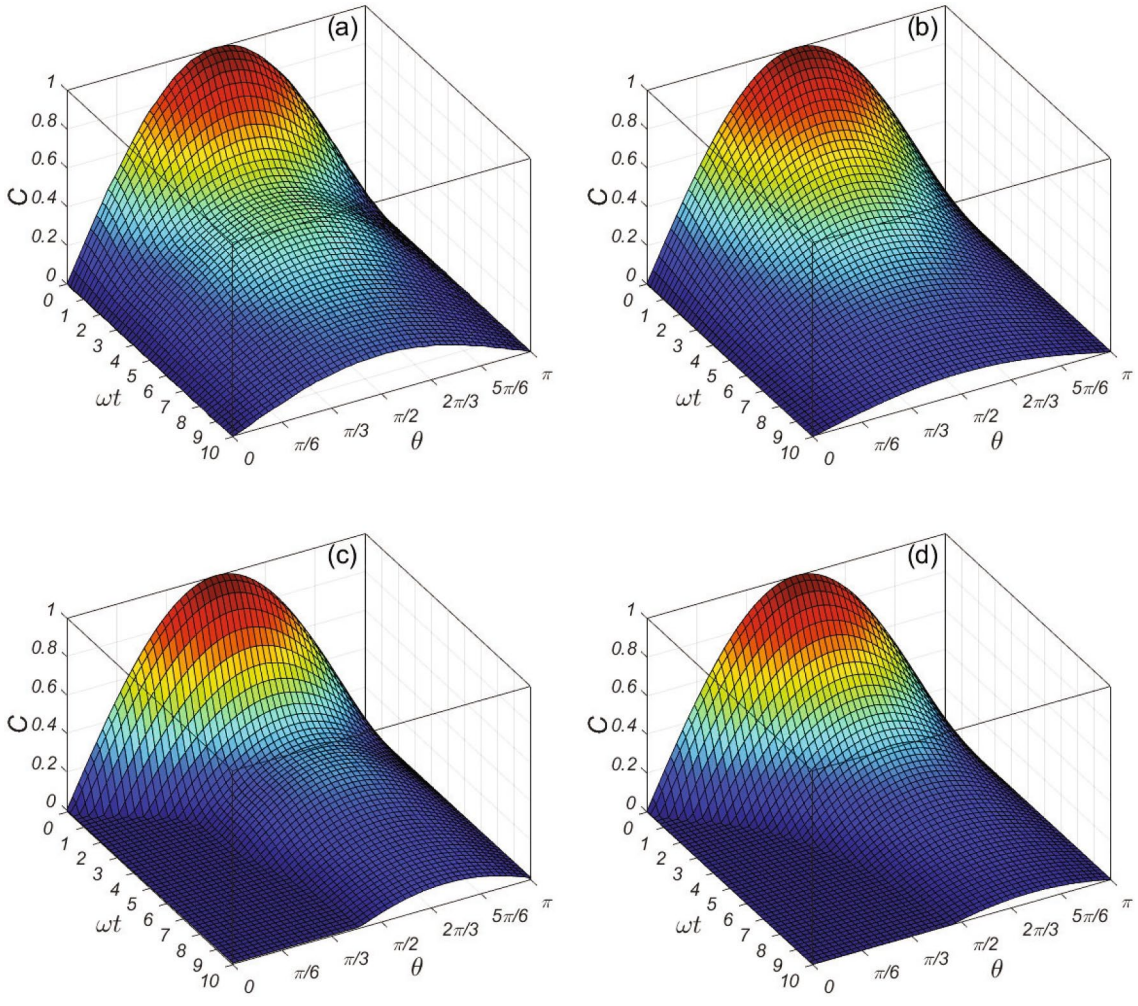

Fig. 4. Time evolution of the concurrence as a function of ωt and θ for distinct initial states under varying noise conditions. (**a**) The initial state $|\Psi_0\rangle = \cos(\theta/2)\,|2\rangle + \sin(\theta/2)\,|3\rangle$, under pure relaxation noise. (**b**) The same initial state as in (**a**), encountering a combination of noises with $\Gamma_\alpha/\omega = \Gamma_{A\alpha}/\omega = \Gamma_{B\alpha}/\omega = 2$. (**c**) The initial state $|\Phi_0\rangle = \cos(\theta/2)\,|1\rangle + \sin(\theta/2)\,|4\rangle$, under pure relaxation noise. (**d**) The same initial state as in (**c**), under mixed noise conditions attributed to $\Gamma_\alpha/\omega = \Gamma_{A\alpha}/\omega = \Gamma_{B\alpha}/\omega = 2$. The remaining parameters are set as $\Gamma_\beta/\omega = \Gamma_{A\beta}/\omega = \Gamma_{B\beta}/\omega = 1$ and $\gamma_\beta/\omega = \gamma_{A\beta}/\omega = \gamma_{B\beta}/\omega = 0.5$.

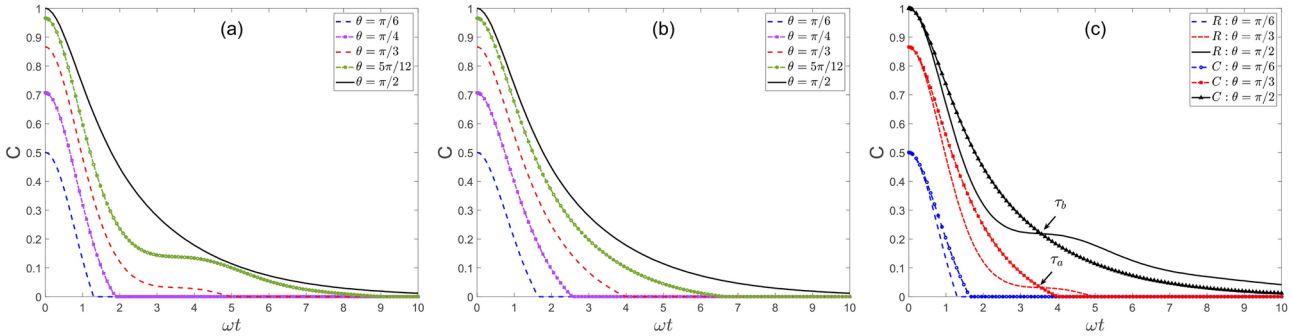

Fig. 5. The time evolution of the concurrence versus ωt with different initial state parameters θ. Here, (**a**) represents the cross sections of Fig. 4c and (**b**) represents the cross sections of Fig. 4d. For straightforward comparison of differences, (**c**) contains the curves in both (**a**) (i.e., curves R under pure relaxation noises) and (**b**) (i.e., curves C under mixture noises).

Scenario	ESD Time	Non-Markovian Effects
Pure relaxation noise Fig. 5a	Increases with θ	No memory effects
Mixed noise conditions Fig. 5b	Increases with θ	Memory effects
Figure 5c ($\theta = \pi/6$)	ESD occurs prior to intersection	Memory effects enhance coherence
Figure 5c ($\theta = \pi/3$)	ESD occurs after intersection	Memory effects enhance coherence ($\omega t < \tau_a$)
Figure 5c ($\theta = \pi/2$)	ESD occurs after intersection	Memory effects enhance coherence ($\omega t < \tau_b$)

Table 1. Summary of the ESD times and non-Markovian effects under different noise conditions.

the parameter θ. Notably, the phase ϕ does not exert an influence on the entanglement dynamics and is thus set to zero for the sake of simplicity and clarity in our analysis. The presence of dephasing noise significantly impacts the ESD time. Specifically, for $\theta > \pi/2$, the probability amplitude of state $|1\rangle$ is less than that of state $|4\rangle$, leading to the absence of ESD. Conversely, for $\theta < \pi/2$, the probability amplitude of state $|1\rangle$ is greater than that of state $|4\rangle$, enabling the occurrence of ESD within this parameter range. For the initial state $|\Psi_0\rangle$, which commences with a non-zero concurrence, the decay of entanglement is gradual, with the entanglement death occurring at an infinite time under ideal conditions, indicating a more robust entanglement against environmental decoherence.

To provide a comprehensive understanding of the intricate dynamics of ESD, we conducted a detailed analysis of the cross-sections illustrated in Fig. 5. The trends in ESD times and non-Markovian effects are summarized in Table 1. These cross-sections depict the time evolution of the concurrence as a function of ωt for the initial states $|\Phi_0\rangle$, with θ as a variable parameter. This analysis offers valuable insights into the relationship between system parameters and the onset of ESD, elucidating the mechanisms that govern the stability of quantum entanglement. In Fig. 5a and b, we observe a consistent trend in ESD time as θ varies. Specifically, within the interval $0 < \theta < \pi/2$, the ESD time increases with θ. This behavior can be attributed to the enhanced resilience of the system's entanglement against decoherence processes as θ increases. Larger values of θ correspond to states that are less susceptible to relaxation, thereby delaying the onset of ESD. This delay results from the system evolving towards a more stable configuration, significantly reducing its vulnerability to entanglement degradation. As θ approaches $\pi/2$, the ESD time asymptotically approaches infinity, indicating a complete suppression of ESD within this parameter regime. This phenomenon can be explained by the system's evolution towards a configuration that is highly resistant to entanglement degradation, effectively preventing the sudden death of quantum correlations.

Figure 5c further explores the influence of dephasing noise on concurrence and the occurrence of ESD. In the moderate time scale $0 < \omega t < \tau$, where τ is the critical time at which the lines labeled R and C intersect (e.g.,in Fig. 5c, the point τ_a for $\theta = \pi/3$ or τ_b for $\theta = \pi/2$), the presence of mixed noises results in a higher concurrence compared to the scenario under purely relaxation noise. This unexpected outcome can be attributed to the Non-Markovian nature of the noise, wherein the system retains memory of its past interactions with the environment. In this regime, dephasing noise partially mitigates the effects of relaxation noise, thereby preserving entanglement to a greater extent. The Non-Markovian dynamics allow the system to exploit its memory of previous states, leading to a temporary enhancement of coherence that counters the immediate effects of relaxation.

Conversely, for the time scale $\omega t > \tau$, the curve under mixed noise experiences ESD more rapidly. This acceleration arises from the combined effects of relaxation and dephasing noise, which, beyond the critical threshold τ, leads to cumulative degradation of entanglement. The absence of intersection of curves for $\theta = \pi/6$ indicates that ESD occurs prior to the intersection, suggesting a delayed ESD time under mixed noises. This delay can be attributed to the intricate interplay between relaxation and dephasing mechanisms, which can either hasten or delay the onset of ESD depending on the specific time scale and system parameters.

Notably, the critical time τ serves as a boundary where the Non-Markovian memory of the environment transitions from protecting the system's coherence to facilitating its degradation. This transition underscores the pivotal role of environmental memory in the dynamics of quantum entanglement, highlighting that while Non-Markovian effects can initially enhance entanglement, they can also lead to more rapid decoherence once a certain threshold is crossed. Thus, the interplay between different types of noise and their temporal characteristics is crucial in understanding the stability and longevity of quantum entanglement in realistic scenarios. Furthermore, the Non-Markovian nature of the noise introduces a temporal correlation that affects the system's response to environmental perturbations. This correlation can lead to a backflow of information from the environment to the system, which in turn can temporarily restore or enhance the system's coherence. This phenomenon is particularly evident in the regime $0 < \omega t < \tau$, where the Non-Markovian effects counteract the detrimental impacts of relaxation noise, leading to an increase in concurrence. However, as the system evolves beyond the critical time τ, the cumulative effect of Non-Markovian noise can exacerbate the degradation of entanglement, leading to a more rapid onset of ESD. This dual role of Non-Markovian noise, both protecting and degrading entanglement, highlights the complex and time-dependent nature of its impact on quantum systems.

Furthermore, the non-Markovian dynamics, characterized by the time-dependent dephasing rates Γ_α, introduce memory effects that can lead to the revival of entanglement even after periods of decay. This is in stark contrast to Markovian dynamics, where the system's evolution is independent of its history. In our system, the non-Markovian nature of the noise is evident in the fluctuating dephasing rates, which are influenced by the system's past interactions with the environment. The presence of non-Markovian effects can be seen in the delayed ESD time under mixed noises, as the complex interplay between relaxation and dephasing mechanisms can either hasten or delay the onset of ESD. For certain parameter regimes, particularly when θ is close to $\pi/2$, the system exhibits a higher resistance to entanglement degradation, which can be attributed to the non-Markovian memory effects that preserve entanglement for longer durations. In the context of the initial states $|\Phi_0\rangle$ and $|\Psi_0\rangle$, the non-Markovian dynamics result in a more nuanced picture of entanglement sudden death. For $|\Phi_0\rangle$, the ESD time is not only dependent on θ but also on the history of the system's evolution, which can affect the rate at which entanglement decays or revives. On the other hand, for $|\Psi_0\rangle$, the gradual decay of entanglement suggests that the non-Markovian effects are less pronounced, allowing for a more robust entanglement against environmental decoherence.

Figure 6 enriches our understanding by exploring the impact of varying environmental parameters on the system's dynamics. Specifically, we consider environments *A* and *B* with differing inversion memory capacity parameters $\gamma_{A\beta}$ and $\gamma_{B\beta}$. By fixing $\gamma_{A\beta}/\omega = 1$ and systematically varying $\gamma_{B\beta}/\omega$ across a range of values (0, 0.1, 0.2, 0.5, and 1), we observe that the concurrence decreases at an accelerated rate as the inversion memory capacity $\gamma_{B\beta}$ increases. This acceleration can be attributed to the enhanced interaction between the system and the environment, leading to faster decoherence rates and a more rapid degradation of entanglement. The increased interaction strength results in a more pronounced effect of the environment on the system, hastening the loss of entanglement. Notably, Non-Markovian noise introduces memory effects that can temporarily preserve coherence; however, as $\gamma_{B\beta}$ increases, the system becomes more susceptible to rapid environmental fluctuations that overwhelm these memory effects. Specifically, while Non-Markovian noise allows for a backflow of information from the environment to the system, counteracting decoherence, high values of $\gamma_{B\beta}$ lead to stronger environmental fluctuations that surpass this coherence preservation, resulting in a faster decay of entanglement. Moreover, the entanglement sudden death (ESD) time is shortened under these conditions, reflecting the accelerated entanglement degradation. Notably, when the inversion memory capacity of a single environment $\gamma_{B\beta}$ approaches 0, the ESD time increases to infinity, even in the presence of a non-zero inversion memory capacity in the other environment (i.e., $\gamma_{A\beta}$). This observation underscores the pivotal role of environmental

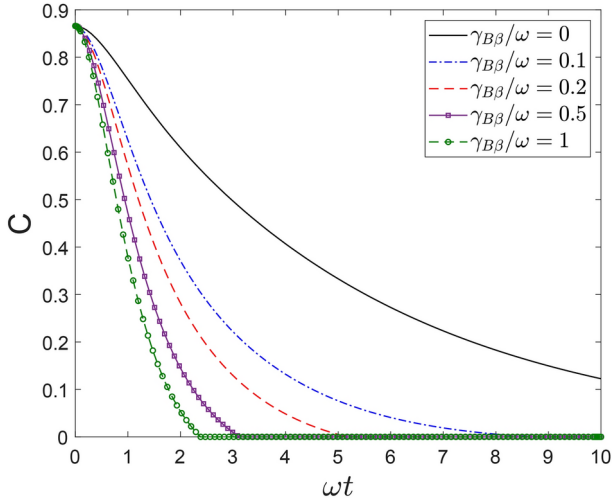

Fig. 6. The time evolution of the concurrence versus ωt with different parameters $\gamma_{B\beta}$. Here we choose other parameters as initial state parameters $\theta = \pi/3$, $\Gamma_{A\beta}/\omega = \Gamma_{B\beta}/\omega = 1$, $\gamma_{A\beta}/\omega = 1$ and $\Gamma_{A\alpha}/\omega = \Gamma_{B\alpha}/\omega = 2$.

parameters in determining the robustness of entanglement against ESD. The interplay between Non-Markovian noise and the system's dynamics highlights the critical importance of managing these parameters in quantum information processing tasks to ensure the longevity and stability of quantum entanglement. By understanding how Non-Markovian effects influence the system's response to environmental changes, we can better design protocols that mitigate the adverse effects of noise, thereby enhancing the fidelity of quantum teleportation.

Conclusions

In conclusion, our research has significantly advanced the field of quantum information science by elucidating the dynamics of entanglement within quantum systems, focusing particularly on the interplay between initial state parameters and environmental influences. We have underscored the critical role of dephasing rates and initial state configurations in determining the robustness and longevity of quantum correlations, which is foundational for developing strategies to protect quantum information against environmental noise. This knowledge is essential for the advancement of quantum technologies, especially in quantum computing, communication, and cryptography, where maintaining quantum coherence and entanglement is crucial. Our detailed analysis has provided a deeper understanding of entanglement sudden death (ESD) dynamics, enabling more precise prediction and control over its onset. This enhanced understanding is pivotal for optimizing quantum systems to ensure stability and functionality over the requisite operational timescales. The insights from this study will be invaluable in guiding future research and development efforts in quantum information science and technology, ensuring that quantum coherence and entanglement can be maintained over longer timescales and under more challenging environmental conditions

Building upon these findings, future research could explore the impact of incorporating a controllable time-varying magnetic field or applying analogous approaches to other open system models, such as cavity quantum electrodynamics and Heisenberg spin chains. This extension will not only deepen our understanding of the underlying physics but also potentially lead to innovative strategies for enhancing quantum coherence and entanglement in practical quantum systems. By skillfully manipulating environmental conditions and system parameters, we can engineer quantum systems that are more resilient to decoherence, paving the way for the realization of practical quantum devices with enhanced performance and reliability.

Data availability

The datasets used and/or analyzed during the current study available from the corresponding author on reasonable request.

Received: 15 July 2024; Accepted: 27 September 2024
Published online: 12 October 2024

References

1. Vaidman, L. Teleportation of quantum states. *Phys. Rev. A* **49**, 1473–1476. https://doi.org/10.1103/PhysRevA.49.1473 (1994).
2. Bennett, C. H. & Wiesner, S. J. Communication via one- and two-particle operators on Einstein–Podolsky–Rosen states. *Phys. Rev. Lett.* **69**, 2881–2884. https://doi.org/10.1103/PhysRevLett.69.2881 (1992).
3. Bennett, C. H. *et al.* Teleporting an unknown quantum state via dual classical and Einstein–Podolsky–Rosen channels. *Phys. Rev. Lett.* **70**, 1895–1899. https://doi.org/10.1103/PhysRevLett.70.1895 (1993).
4. Wiseman, H. M. & Milburn, G. J. *Quantum Measurement and Control* (Cambridge University Press, Cambridge, 2009).
5. Bellomo, B., Lo Franco, R. & Compagno, G. Non-Markovian effects on the dynamics of entanglement. *Phys. Rev. Lett.* **99**, 160502. https://doi.org/10.1103/PhysRevLett.99.160502 (2007).
6. Bellomo, B., Lo Franco, R. & Compagno, G. Entanglement dynamics of two independent qubits in environments with and without memory. *Phys. Rev. A* **77**, 032342. https://doi.org/10.1103/PhysRevA.77.032342 (2008).
7. Fanchini, F. F., Werlang, T., Brasil, C. A., Arruda, L. G. E. & Caldeira, A. O. Non-Markovian dynamics of quantum discord. *Phys. Rev. A* **81**, 052107. https://doi.org/10.1103/PhysRevA.81.052107 (2010).
8. de Vega, I. & Alonso, D. Dynamics of non-Markovian open quantum systems. *Rev. Mod. Phys.* **89**, 015001. https://doi.org/10.1103/RevModPhys.89.015001 (2017).
9. Basit, A., Ali, H., Badshah, F. & Ge, G.-Q. Enhancement of quantum correlations in qubit-qutrit systems under the non-Markovian environment. *Commun. Theor. Phys.* **68**, 29. https://doi.org/10.1088/0253-6102/68/1/29 (2017).
10. Yang, H., Miao, H. & Chen, Y. Nonadiabatic elimination of auxiliary modes in continuous quantum measurements. *Phys. Rev. A* **85**, 040101. https://doi.org/10.1103/PhysRevA.85.040101 (2012).
11. Chen, Y., Ding, Q., Shi, W., Jun, J. & Yu, T. Exact entanglement dynamics mediated by leaky optical cavities. *J. Phys. B: At. Mol. Opt. Phys.* **53**, 125501. https://doi.org/10.1088/1361-6455/ab707c (2020).
12. Shor, P. W. Scheme for reducing decoherence in quantum computer memory. *Phys. Rev. A* **52**, R2493–R2496. https://doi.org/10.1103/PhysRevA.52.R2493 (1995).
13. Shor, P. & Laflamme, R. Quantum analog of the MacWilliams identities for classical coding theory. *Phys. Rev. Lett.* **78**, 1600–1602. https://doi.org/10.1103/PhysRevLett.78.1600 (1997).
14. Lidar, D. A., Chuang, I. L. & Whaley, K. B. Decoherence-free subspaces for quantum computation. *Phys. Rev. Lett.* **81**, 2594–2597. https://doi.org/10.1103/PhysRevLett.81.2594 (1998).
15. Ladd, T. D. *et al.* Quantum computers. *Nature* **464**, 45–53. https://doi.org/10.1038/nature08812 (2010).
16. Kwiat, P. G., Berglund, A. J., Altepeter, J. B. & White, A. G. Experimental verification of decoherence-free subspaces. *Science* **290**, 498–501. https://doi.org/10.1126/science.290.5491.498 (2000).
17. Xu, J.-S. *et al.* Experimental investigation of classical and quantum correlations under decoherence. *Nat. Commun.* **1**, 7. https://doi.org/10.1038/ncomms1005 (2010).
18. Viola, L., Knill, E. & Lloyd, S. Dynamical decoupling of open quantum systems. *Phys. Rev. Lett.* **82**, 2417–2421. https://doi.org/10.1103/PhysRevLett.82.2417 (1999).
19. Yi, X. & Sun, C. Factoring the unitary evolution operator and quantifying entanglement. *Phys. Lett. A* **262**, 287–295 (1999).
20. Strunz, W. T. & Yu, T. Convolutionless non-Markovian master equations and quantum trajectories: Brownian motion. *Phys. Rev. A* **69**, 052115. https://doi.org/10.1103/PhysRevA.69.052115 (2004).
21. Preskill, J. Quantum computing in the NISQ era and beyond. *Quantum* **2**, 79. https://doi.org/10.22331/q-2018-08-06-79 (2018).

22. Li, C.-F., Guo, G.-C. & Piilo, J. Non-Markovian quantum dynamics: What does it mean?. *Europhys. Lett.* **127**, 50001. https://doi.org/10.1209/0295-5075/127/50001 (2019).
23. Puente, D. A., Motzoi, F., Calarco, T., Morigi, G. & Rizzi, M. Quantum state preparation via engineered ancilla resetting. *Quantum* **8**, 1299. https://doi.org/10.22331/q-2024-03-27-1299 (2024).
24. Zhang, K. *et al.* Reconfigurable hexapartite entanglement by spatially multiplexed four-wave mixing processes. *Phys. Rev. Lett.* **124**, 090501. https://doi.org/10.1103/PhysRevLett.124.090501 (2020).
25. Dakir, Y., Slaoui, A., Mohamed, A.-B.A., Laamara, R. A. & Eleuch, H. Quantum teleportation and dynamics of quantum coherence and metrological non-classical correlations for open two-qubit systems. *Sci. Rep.* **13**, 20526. https://doi.org/10.1038/s41598-023-46396-2 (2023).
26. Pan, Y., Xi, Z.-R. & Gong, J. Optimized dynamical decoupling sequences in protecting two-qubit states. *J. Phys. B: At. Mol. Opt. Phys.* **44**, 175501. https://doi.org/10.1088/0953-4075/44/17/175501 (2011).
27. Chaudhry, A. Z. & Gong, J. Decoherence control: Universal protection of two-qubit states and two-qubit gates using continuous driving fields. *Phys. Rev. A* **85**, 012315. https://doi.org/10.1103/PhysRevA.85.012315 (2012).
28. Mohamed, A.-B., Eleuch, H. & Ooi, C. R. Non-locality correlation in two driven qubits inside an open coherent cavity: Trace norm distance and maximum bell function. *Sci. Rep.* **9**, 19632. https://doi.org/10.1038/s41598-019-55548-2 (2019).
29. Mohamed, A.-B.A., Abdel-Aty, A.-H., Qasymeh, M. & Eleuch, H. Non-local correlation dynamics in two-dimensional graphene. *Sci. Rep.* **12**, 3581. https://doi.org/10.1038/s41598-022-07204-5 (2022).
30. Shu, W., Zhao, X., Jing, J., Wu, L.-A. & Yu, T. Uhrig dynamical control of a three-level system via non-Markovian quantum state diffusion. *J. Phys. B: At. Mol. Opt. Phys.* **46**, 175504. https://doi.org/10.1088/0953-4075/46/17/175504 (2013).
31. Man, Z.-X., Xia, Y.-J. & Lo Franco, R. Cavity-based architecture to preserve quantum coherence and entanglement. *Sci. Rep.* **5**, 13843. https://doi.org/10.1038/srep13843 (2015).
32. Szańkowski, P., Ramon, G., Krzywda, J., Kwiatkowski, D. & Cywiński, Ł. Environmental noise spectroscopy with qubits subjected to dynamical decoupling. *J. Phys.: Condens. Matter* **29**, 333001. https://doi.org/10.1088/1361-648x/aa7648 (2017).
33. Chen, Y., You, J. Q. & Yu, T. Exact non-Markovian master equations for multiple qubit systems: Quantum-trajectory approach. *Phys. Rev. A* **90**, 052104. https://doi.org/10.1103/PhysRevA.90.052104 (2014).
34. Jing, J., Yu, T., Lam, C.-H., You, J. Q. & Wu, L.-A. Control relaxation via dephasing: A quantum-state-diffusion study. *Phys. Rev. A* **97**, 012104. https://doi.org/10.1103/PhysRevA.97.012104 (2018).
35. Hosseiny, S. M., Seyed-Yazdi, J., Norouzi, M. & Livreri, P. Quantum teleportation in Heisenberg chain with magnetic-field gradient under intrinsic decoherence. *Sci. Rep.* **14**, 9607. https://doi.org/10.1038/s41598-024-60321-1 (2024).
36. Losada, M., Bosyk, G. M., Freytes, H. & Sergioli, G. Transformations of superpositions by means of incoherent operations. *Sci. Rep.* **10**, 8245. https://doi.org/10.1038/s41598-020-63661-w (2020).
37. Xu, Z.-J. & An, J.-H. Noise mitigation in quantum teleportation. *Phys. Rev. A* **110**, 012442. https://doi.org/10.1103/PhysRevA.110.012442 (2024).
38. Wootters, W. K. Entanglement of formation of an arbitrary state of two qubits. *Phys. Rev. Lett.* **80**, 2245–2248. https://doi.org/10.1103/PhysRevLett.80.2245 (1998).
39. Cai, X. Quantum dephasing induced by non-Markovian random telegraph noise. *Sci. Rep.* **10**, 88. https://doi.org/10.1038/s41598-019-57081-8 (2020).
40. Horodecki, R., Horodecki, P., Horodecki, M. & Horodecki, K. Quantum entanglement. *Rev. Mod. Phys.* **81**, 865–942. https://doi.org/10.1103/RevModPhys.81.865 (2009).
41. Amico, L., Fazio, R., Osterloh, A. & Vedral, V. Entanglement in many-body systems. *Rev. Mod. Phys.* **80**, 517–576. https://doi.org/10.1103/RevModPhys.80.517 (2008).
42. Diósi, L., Gisin, N. & Strunz, W. T. Non-Markovian quantum state diffusion. *Phys. Rev. A* **58**, 1699–1712. https://doi.org/10.1103/PhysRevA.58.1699 (1998).
43. Yu, T., Diósi, L., Gisin, N. & Strunz, W. T. Non-Markovian quantum-state diffusion: perturbation approach. *Phys. Rev. A* **60**, 91–103. https://doi.org/10.1103/PhysRevA.60.91 (1999).
44. Diósi, L. & Strunz, W. T. The non-Markovian stochastic Schrödinger equation for open systems. *Phys. Lett. A* **235**, 569–573 (1997).
45. Breuer, H.-P., Kappler, B. & Petruccione, F. Stochastic wave-function method for non-Markovian quantum master equations. *Phys. Rev. A* **59**, 1633–1643. https://doi.org/10.1103/PhysRevA.59.1633 (1999).

Acknowledgements

This work is supported by National Natural Science Foundation of China (U2330109, 62405239, 61805212, 51802245, 61405151, 11604252), National Key Laboratory of Plasma Physics (6142A04230302), Natural Science Foundation of Shaanxi Province (2022JQ-660, 2020JQ-830, 20180418), Key Research and Development Program of Shaanxi Province (2024GX-YBXM-081, 2023-YBGY-196), Shaanxi Fundamental Science Research Project for Mathematics and Physics (22JSY030, 22JSY012), Special Scientific Research Project in Shaanxi Province Department of Education (20JK0662, 21JK0653) and Space Optoelectronic Measurement and Perception Lab Beijing Institute of Control Engineering (LabSOMP-2023-01).

Author contributions

H.Z. conceived the study and wrote the manuscript. X.H., G.Z., L.L., L.C., J.W., Y.Z., Y.X. and C.X. analyzed the results. All authors reviewed the manuscript.

Competing interests

The authors declare no competing interests.

Additional information

Correspondence and requests for materials should be addressed to C.X.

Reprints and permissions information is available at www.nature.com/reprints.

Publisher's note Springer Nature remains neutral with regard to jurisdictional claims in published maps and institutional affiliations.